Food Bioscience 59 (2024) 103912

Contents lists available at ScienceDirect

Food Bioscience

journal homepage: www.elsevier.com/locate/fbio

Drying kinetics modeling of hot air drying of emulsion templated oleogels employing hydroxypropyl methylcellulose as structuring agent

M.Y. Saavedra, L. Montes, D. Franco, A. Franco-Uría, R. Moreira *

Department of Chemical Engineering, Universidade de Santiago de Compostela, rúa Lope Gómez de Marzoa, s/n. 15782, Santiago de Compostela, Spain

ARTICLE INFO

Keywords:
Critical moisture content
Oil binding capacity
Storage
Sunflower oil
Texture

ABSTRACT

This work focused on the drying of O/W emulsions employed to obtain templated structured oils with hydroxypropyl methylcellulose (HPMC) as oleogelator. Sunflower oil/water emulsions with different HPMC content (1%–3% w/w) were dried at different air temperatures (from 70 to 100 °C) employing two different initial thicknesses (0.25 and 0.50 cm). Drying kinetics showed the existence of an initial constant drying rate period followed by a falling drying rate period below critical moisture content. This critical content was constant (0.38 kg water/kg dry solid) independently of drying conditions and HPMC content. Drying rate decreased linearly with moisture content during the falling rate periods. A 3-parameter model was proposed to simulate drying kinetics in the range of drying temperature and HPMC content of tested oleogels. Physical properties of fresh and stored (20 days) oleogels such as oil binding capacity, color, and hardness were measured to evaluate drying conditions effect on product quality. Temperatures above 70 °C were necessary to promote the HPMC gelation. Best characteristics of oleogels in terms of texture, color and oil binding capacity were obtained with HPMC content of 2% w/w, 0.25 cm of emulsion thickness and 80 °C of drying temperature. These results are useful for the design of large-scale dryers for this new kind of products.

1. Introduction

Functional lipids and nutritional improvement of lipid-containing foods have gained more and more interest since recent regulations banned the use of artificial trans fatty acids (TFA) and several entities suggested the limitation of saturated fatty acids (SFA) in foods (Manzoor et al., 2022). The current practice in the food industry to manage TFA issues is the replacement of these acids with natural SFA, generally obtained by the fractionation of different fats of tropical origin, mainly, palm oil. However, the use of palm oil as the main source of SFA might affect both the consumers' health and the environment (Gatti et al., 2019). Therefore, there is a real need for healthier, TFA-free, stable, and solid-like fats, which maintain their structure at ambient temperature (20 °C), assuring a longer shelf-life (Puscas et al., 2020).

From a research perspective, oleogelation has been proposed as an alternative oil structuring strategy that may help formulate food products without a significant amount of SFA. The emulsion-template approach involves the preparation of an emulsion stabilized by a hydrophilic gelator, followed by the removal of the hydrophilic solvent. The result is a dried structure, where the hydrophilic gelator network acts as a building block for the oil fraction, forming an oleogel (Patel, 2015). Cellulose derivatives such as methylcellulose (MC), hydroxypropyl methylcellulose (HPMC) and carboxymethylcellulose (CMC) are used in oil structuring applications by the emulsion-based approach (Jiang et al., 2018; Oh & Lee, 2018). HPMC is a surface-active amphiphilic biopolymer that can be adsorbed onto the oil droplets, protecting them, thus decreasing the amount of oil available for separation (Bascuas et al., 2021). Cellulose derivatives are first hydrated in an aqueous solution. Then, the oil-in-water emulsion is prepared (template) and stabilized by the amphiphilic polymers adhered to the oil surface and formed a layer to coat the oil droplet. Water is removed to drive the structure formation by the interaction among polysaccharides mainly via hydrogen bonding during dehydration process to trap the oil. (Huang et al., 2023). Therefore, a structured network encapsulating the liquid oil is formed during dehydration. Finally, the dried product is homogenized to obtain an oleogel.

Water removal from O/W emulsions can be performed with different methods, like for example freeze-drying and supercritical CO_2 drying

* Corresponding author. Department of Chemical Engineering, Universidade de Santiago de Compostela, rúa Lope Gómez de Marzoa, Santiago de Compostela, E-15782, Spain.
E-mail address: ramon.moreira@usc.es (R. Moreira).

https://doi.org/10.1016/j.fbio.2024.103912
Received 12 October 2023; Received in revised form 12 March 2024; Accepted 14 March 2024
Available online 15 March 2024
2212-4292/© 2024 The Authors. Published by Elsevier Ltd. This is an open access article under the CC BY license (http://creativecommons.org/licenses/by/4.0/).

(Jiang et al., 2018; Jung et al., 2023; Li et al., 2023; Pan et al., 2021; Xu et al., 2023), although hot air drying is also the selected method in other works, either with natural (Alizadeh et al., 2020; Espert et al., 2020) or forced convection (Wang et al., 2023; Álvarez et al., 2021). The drying process of the emulsion is an important step in oleogel formation, and several authors analyzed the influence of the drying method on the properties of oleogels (Bascuas et al., 2020; Chen & Yang, 2019; Qiu et al., 2018). For instance, Bascuas et al. (2020) concluded that both conventional and vacuum drying resulted in oleogels with adequate structure when employing olive and sunflower oil, while those oleogels using linseed oil presented a poor structure with the independence of the drying method. Additionally, vacuum drying seemed to prevent oxidation of oleogels during storage. In other study, Qiu et al. (2018) compared freeze-drying and conventional drying of emulsions stabilized with several gelatin-polyphenol-polysaccharides complexes. Their results showed that the air-dried oleogels presented a softer, more-spreadable texture than the freeze-dried samples, due to the different mechanisms of water removal. Similar results were found by Chen and Yang (2019). Freeze-dried and vacuum-oven dried oleogels were compared by Moradabbasi et al. (2022). While a better texture and mechanical strength were found in the freeze-dried oleogels, oxidative stability was similar employing both drying methods. Abdolmaleki et al. (2020) also found that in general, freeze-dried oleogels presented higher oil binding capacity and structure recovery values.

Despite these relevant contributions, there are no studies focusing on the hot air-drying kinetics of oleogels, dealing with variables such as drying temperature, emulsion thickness, organogelator concentration, as these independent variables significantly can affect final oleogel properties (i.e hardness, oil retention, color, oxidative level, rheology, among others). Therefore, the objective of this study was to determine the drying kinetics of sunflower emulsions with HPMC at different temperatures (70–100 °C), different thicknesses during the drying stage (0.25–0.50 cm), and different concentrations of the organogelator (1%–3%), and to assess their effect on the texture, color, and oil binding capacity (OBC) in the resulting oleogel. As far as we know, this specific objective is the first time proposed in the promising field of oil structuring.

2. Materials and methods

2.1. Materials

HPMC with a viscosity of 80–120 cP in 2% aqueous solution at 20 °C was purchased from Sigma-Aldrich Company (St. Louis, MO, USA). Sunflower oil was kindly supplied by a local company (Aceites Abril, S. L., Ourense, Spain). Composition of sunflower oil determined according to CODEX Stan 210 normative (Codex Alimentarius, 2005) was provided by the supplier company; it was: acidity (0.09%), peroxide value (0.43 meq O_2/kg), moisture (<0.1%) and impurities (<0.05%). The fatty acid profile (% w/w) of sunflower oil also provided by the supplier and determined using standard official methods was in percentage: myristic acid (0.07), palmitic acid (3.62), palmitoleic acid (0.13), stearic acid (3.32), oleic acid (31.03), linoleic (57.6), linolenic (0.08), arachidic acid (0.25), behenic acid (0.73), and lignoceric acid (0.26). Chromatic parameters of refined sunflower oil were L* = 37.25 ± 0.56; a* = 0.21 ± 0.03; b* = 1.84 ± 0.02).

2.2. Preparation of emulsions

Based on the protocol described by Espert et al. (2021), the oil in water emulsions were prepared with slight modifications focused on the drying stage. The composition of the initial oil in water emulsion was 50% (w/w) sunflower oil, HPMC at different concentrations (1%, 2% and 3%) and cold deionized water up to 100%. The aqueous HPMC solution previously prepared was added to sunflower oil in a 200 ml beaker using a stirrer of 2.5 cm 4-blade (IKA-WERK RW 20 DZM, Staufen, Germany) at 280 rpm for 5 min. Subsequently, chilled water (~10 °C) was incrementally introduced while maintaining continuous stirring for 30 s. At this point, the amount of emulsion prepared was dependent on the dimensions of the designated tray to achieve the desired thickness. Finally, the emulsion was homogenized in a high-energy dispersion unit (Ultraturrax T-25 Basic, IKA-WERK, Staufen, Germany) at 6500 rpm for 15 s followed by a second phase at 17500 rpm for 60 s.

2.3. Drying of emulsions

Once the emulsions were prepared, they were rested for 20 min at room temperature (20 °C). Afterwards, the emulsions were poured into foil trays and introduced into a forced convective air dryer (Angelantoni Challenge 250, Massa Martana, Italy) for moisture removal until a gelled solid was obtained. All samples were dried at constant weight (final moisture content less than 0.01 kg water/kg d.s.). The experiments were performed at four temperatures (70, 80, 90 and 100 °C) and at two emulsion thicknesses (0.25 and 0.50 cm). Constant air velocity (2 m/s) and relative humidity (10%) of air were maintained constant in the dryer. Drying kinetics (n = 2) were obtained by weight monitoring every 20 min in a precision balance (Mettler Toledo PJ3000, Coslada, Spain).

The equilibrium moisture content of oleogels was assumed zero in all the experiments. This value is justified by the air conditions employed during the experiments (high temperature and low relative humidity of air), together with the fact of the hydrophobic nature of main component (oil). Drying rates, $-dX/dt$ (kg water/(kg d.s.·min)), were evaluated for each experiment, and plotted vs absolute moisture X (kg water/kg d.s.) of solid sample. This representation allows identifying better the existence of the falling and constant rate periods, and eventually the critical moisture content determination. Superficial liquid water is evaporated during the constant rate period, being the drying rate described by Eq. (1) under constant external air conditions:

$$-\frac{dX}{dt} = k \tag{1}$$

being k (kg water/(kg d.s.·min)) the drying rate constant.

Eq. (2) can be used when it is assumed that this decrease is linear:

$$-\frac{dX}{dt} = K\,(X - X_e) = K\,X \tag{2}$$

where X_e (kg water/kg d.s.) is the equilibrium moisture (zero in our case) and K (min^{-1}) is the rate constant for the falling rate period.

Water evaporation rates (E) in g water/min were determined in trays filled only with water at the tested temperatures (70, 80, 90 and 100 °C). The objective of these additional experiments was to compare the specific evaporation rates obtained for the constant rate period during the drying of the emulsions with those of pure water. These results are shown in Table S1 (Supporting Information, S·I.).

2.4. Oleogel preparation

Before obtaining the oleogel, dried emulsion was left to rest for 30 min and then was ground and homogenized at room temperature (20 °C) with a 150 W power blade mill (Severin KM 3879, Sundern, Germany) in eight cycles of 5 s, to obtain a homogeneous paste. Finally, the oleogel formed was placed in 20 × 30 mm plastic ice trays which they were kept refrigerated at 4 °C for 2 h before carrying out the oleogel characterization analyzes (oil binding capacity, texture, and color).

2.5. Oil binding capacity (OBC)

The OBC was assessed following a centrifuge test following the protocol proposed by Okuro et al. (2018) with slight modifications. Briefly, oleogel samples (1 g) were weighed into Eppendorf tubes and subjected to centrifugation in a minicentrifuge (HWLAB, HW12, Shiley,

NW, USA) at 12,500×*g* for 25 min at 20 °C. After centrifugation, the excess liquid oil was removed as a supernatant with a Pasteur pipette and then the Eppendorf tube was weighed again with the sample. The percentage of OBC was calculated using Eq. (3):

$$OBC\ (\%) = \left[1 - \frac{(m1 - m) - (m2 - m)}{(m1 - m)}\right] \times 100 \quad (3)$$

where m (g) is the weight of the empty Eppendorf tube, m1 (g) weight of the Eppendorf tube with oleogel sample before centrifugation and m2 (g) is the weight of the Eppendorf tube with oleogel after centrifugation and oil drainage.

2.6. Textural properties

The textural properties of oleogels were assessed following the procedure proposed by Espert et al. (2020). Oleogel samples (average dimensions 28 × 29 × 11 mm) were compressed using a texturometer (TA. XT Plus, Stable Micro Systems, Surrey, UK), fitted with a 5 kg load cell. The compression test was carried out with a 6 mm diameter SMS P/6 cylindrical probe, compressing the oleogel up to 6 mm, setting an activation force (threshold) of 0.5 g. The speed (mm/s) of pre-test, test and post-test used in all experiments were 1, 1 and 10, respectively. For each oleogel batch, a total of 6 replicates were evaluated. Maximum hardness force (N) by compression, which indicates the oleogel firmness, total necessary work (N m) performed to compress the oleogel (indicates the energy necessary to compress or reduce the volume of the oleogel when an external force is applied) and the elasticity modulus (N/m) which indicates the relationship between the effort and the deformation were obtained.

2.7. Color features

A portable colorimeter (Konica Minolta CR-300, Osaka, Japan) was used to measure the oleogel color in the CIELAB space (lightness, L*; redness, a*; yellowness, b*). For each oleogel batch, four measurements were performed, spreading the oleogel samples in Petri dish to obtain homogeneous and representative areas.

To establish the color stability of oleogel after a period of storage, ΔE parameter was evaluated, according to Eq. (4):

$$\Delta E^* = \sqrt{\left(L_1^* - L_2^*\right)^2 + \left(a_1^* - a_2^*\right) + \left(b_1^* - b_2^*\right)} \quad (4)$$

where L_1 and L_2 are lightness at time 0 and 21 days, respectively, a_1 and a_2 are redness at time 0 and 21 days, respectively, and b_1 and b_2 the yellowness, respectively.

2.8. Statistical analysis

An analysis of variance (ANOVA) using the General Linear Model (GLM) procedure of the SPSS package (SPSS 23.0, Chicago, IL, USA) was performed for all dependent variables in the study (OBC, textural and color parameters). Independent variables (temperature, emulsion thicknesses and HPMC concentration) were used in the model. The least squares means were separated using Duncan's test for a significance level $P < 0.05$.

3. Results and discussion

3.1. Drying kinetics

Fig. 1 shows the drying kinetics of oleogels at different HPMC content and temperatures. Independently of tested temperature, at the beginning of the drying, moisture content decreased rapidly at a constant rate. After a certain period (which in turn depended on the drying temperature) the corresponding drying rates fell. At the start, liquid water present on the surface of the emulsion was rapidly evaporated at an individual constant rate (depending on at least drying temperature). After given drying time, a gelled solid was gradually formed at the surface. This phenomenon is called superficial hardening, and it constitutes a barrier to moisture migration. When the hardening was formed, moisture removal started to decrease slower, due to the free water disappeared from the upper surface and free water within the gel must diffuse after evaporation through the gelled layer.

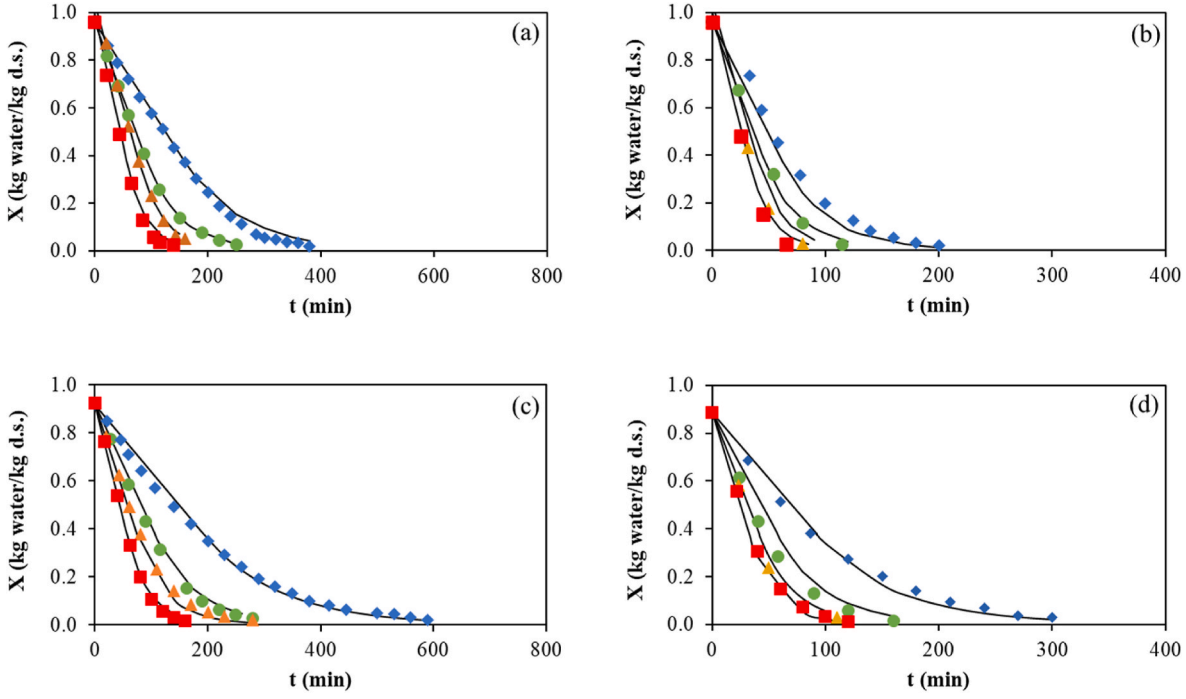

Fig. 1. Experimental (dots) and modelled (lines) air-drying kinetics at several temperatures (°C, 70 ♦,80 ●,90 ▲,100 ■) for oleogels with different HPMC content (% w/w) of 1 (a and b), 2 (c) and 3 (d) and emulsion thickness (0.50 (a and c) and 0.25 cm (b and d)).

In all cases, drying time increased as the air-drying temperature diminished (Fig. 1). For example, with the thinner thickness (0.25 cm) and 1% w/w of HPMC content varied from 75 to 200 min for 100 and 70 °C, respectively, and with thicker thickness (0.50 cm) drying times increased up to 140 and 360 min at the same conditions. This result was expected and reported in many studies for different products (Korese et al., 2021; Kowalski et al., 2017; Singh & Pandey, 2012). At high drying temperatures, the removal of surface moisture (water evaporation) is promoted together with higher water diffusion in the bulk of the oleogel.

Fig. 2 shows the specific drying rate curves for some tested systems, where the limit between the constant rate and falling rate periods could be clearly identified. This point is defined by the critical moisture, X_c, plotted as a vertical line in Fig. 2. It can be seen in Fig. 2 that all the systems present a constant value for X_c equal to 0.38 kg water/kg d.s. During drying experiments, it was observed that the critical time, when the X_c was achieved, was coincident with the apparition of a surface-gelled layer in the emulsion.

In Table 1, the values of k (Eq. (1)) for the constant rate period are shown for all the studied oleogels. It can be observed that the values of the drying rates, at constant HPMC concentration, increased with temperature, resulting in lower drying times, as previously stated. This fact was also reported for emulsion drying by other researchers (Patel et al., 2014; Zheng et al., 2023). Although high temperature accelerates the drying process can modify oleogels properties, and consequently it must be carefully selected since, if the drying temperature is too high, it might result in increased oil oxidation and stability loss, as observed in both studies.

Regarding the effect of HPMC concentration on the constant drying rate, it can be concluded that as concentration increased, the rate decreased (Table 1). For example, at 70 °C and 0.5 cm of thickness, the constant drying rates (kg water/kg d.s.·min) were 0.0037, 0.0027 and 0.0020 at 1%, 2% and 3% w/w of HPMC content, respectively. Therefore, HPMC content had a significant influence on the constant rate, since, as the concentration increased, so did the emulsion viscosity (observed during emulsion preparation). In addition, when HPMC content was higher, the immobilization of the water-oil phase in the network of self-assembled molecules increased (Espert et al., 2020). This is due to the capacity of HPMC to retain water in its molecular structure, affecting the water evaporation rate (Perfetti et al., 2012).

Table 1
Experimental value of drying rate[a], k (kg water/(kg d.s. min)) of Eq. (1), during constant rate period at different temperatures, HPMC content and thickness.

Temperature (°C)	HPMC content (% w/w)	thickness 0.50 cm	thickness 0.25 cm
70	1	0.0037	0.0095
	2	0.0027	0.0072
	3	0.0020	0.0049
80	1	0.0064	0.0152
	2	0.0048	0.0111
	3	0.0041	0.0096
90	1	0.0086	0.0165
	2	0.0071	0.0141
	3	0.0061	0.0131
100	1	0.0110	0.0197
	2	0.0096	0.0175
	3	0.0081	0.0145

[a] SD of ±0.00045.

The drying rate was also affected by emulsion thickness. In Fig. 2 it can be seen how the drying rate was significantly higher in the experiments carried out at 0.25 cm than those developed at 0.50 cm of thickness. If the product to be dried is thick (and/or dense), migration of water molecules to the surface can be hindered (Goavec et al., 2018). Thus, in the samples of 0.5 cm of thickness, mass transfer can be affected since free water has to pass through a higher distance to reach the surface. It must be also considered that the specific interphase (in m^2/m^3 or m^2/kg of material) between air-emulsion (or gelled solid) increases as thickness decreases, improving heat and mass transfer (Xiao et al., 2015).

As expected, specific water evaporation rate increased proportionally with temperature, for both pure water and tested emulsions (Table S1). Also, E was significantly lower in the experiments of emulsion drying since the effective area for water evaporation is reduced due

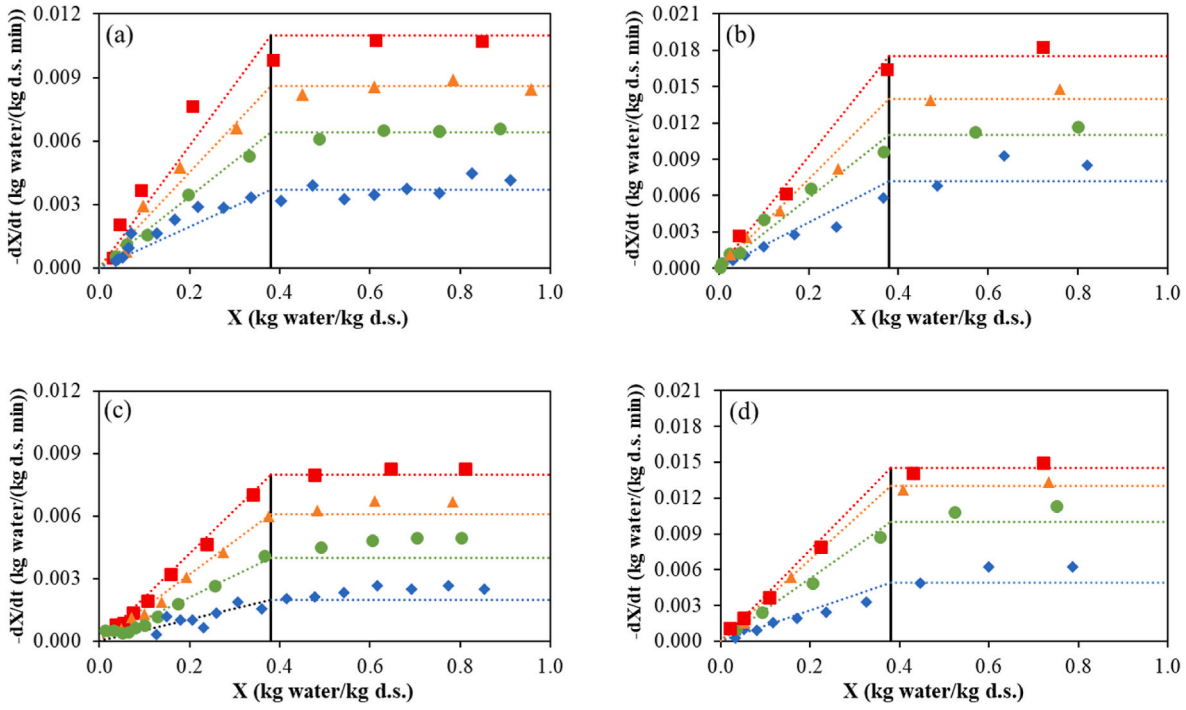

Fig. 2. Experimental (dots) and modelled (lines) specific drying rates at several temperatures (°C, 70 ♦,80 ●,90 ▲,100 ■) for oleogels with different HPMC content (% w/w) of 1 (a), 2 (b) and 3 (c and d) and emulsion thickness (0.50 (a and c) and 0.25 cm (b and d)).

to the presence of the other compounds of the emulsions (mostly oil) on the surface. In example, for those experiments performed at 70 °C, the specific water evaporation rate (g water/(m^2 min)) for the emulsions ranged between 9.86 and 6.55 while for pure water increased up to 41.20. To verify the effect of, in addition to the presence of oil, the concentration of HPMC on the reduction of E (water/oil ratio was constant in all experiments), the percentual decrease of E values with respect to pure water were averaged for each HPMC concentration. The results indicated that, independently of drying temperature, water removal rate was reduced to 28.3 ± 6.2, 25.9 ± 1.9 and 23.5 ± 6.5 for HPMC concentrations of 1%, 2% and 3%, respectively. These values confirmed that water evaporation rate decreased as HPMC concentration increased, due to the decrease in the effective area for evaporation in the emulsion together with the higher capacity of HPMC by its hydrophilic character to retain water in the emulsion as its concentration increased.

During the falling rate period, with limits between [X_e, 0] and [X_c, k], the drying rate decreased linearly in all performed experiments (Fig. 2). The equilibrium moisture content was negligible (as above mentioned) due to the very hydrophobic character of sunflower oil, the main component of the gelled solid obtained at the end of the drying operation. Linear decay can be explained by the gradual formation of a gelled layer. As drying elapses, the thickness of this layer increases (Goavec et al., 2018), and the drying rate falls. Thus, it might be thought that the drying rate decreases proportionally to the growing thickness of the gelled layer, following the basic principles of diffusion (Fick's law). The latter studies observed however a third nonlinear stage in the drying process, but three main differences with respect to the present study need to be considered: i) the nature of the emulsion (alkyl resin and silicone), the drying temperature (normal ambient temperatures around 20 °C) and the thicknesses of the emulsion samples (higher than 1 cm).

3.2. Drying modelling

Modelling provides more insight into the driving mechanisms of the different periods of emulsion drying. Mass and heat transfer modelling was also applied to the experiments for determining pure water evaporation rate, to corroborate the experimental results obtained. This information about water evaporation rates is shown in the S.I. (Table S1).

3.2.1. Emulsions drying

It can be observed in Fig. 3 that the constant drying rate, k (Eq. (1)), was successfully fitted by linear relationships ($R^2 > 0.95$) with drying temperature at constant HPMC content and thickness, Eq. (5):

$$-\frac{dX}{dt} = s\,T - b \tag{5}$$

Slope, s (kg water/(kg d.s. min °C)) values slightly decreased in a narrow range as HPMC concentration raised from 1% to 3% w/w (Table 2). With these results, it was possible to obtain an average value of the slope for each thickness, being $2.25{\cdot}10^{-4}$ and $3.35{\cdot}10^{-4}$ kg water/(kg d.s. min °C) for 0.50 and 0.25 cm of thickness, respectively.

Table 2
Values of s and b, Eq. (5), at different temperatures, HPMC content and thicknesses.

Thickness (cm)	HPMC content (% w/w)	$s\,10^4$ (kg water/(kg d.s min °C))	R^2	b (kg water/(kg d.s. min)
0.50	1	2.41 ± 0.10	0.999	0.01167 ± 0.0005
	2	2.23 ± 0.11	0.999	0.01310 ± 0.0006
	3	2.01 ± 0.09	0.999	0.01407 ± 0.0009
0.25	1	3.44 ± 0.04	0.999	0.01415 ± 0.0006
	2	3.39 ± 0.04	0.999	0.01605 ± 0.0004
	3	3.32 ± 0.03	0.953	0.01788 ± 0.0007

The effect of HPMC content on the constant drying rate was considered in the parameter b of Eq. (5), obtaining its values through variable optimization using the Solver tool of Ms Excel. Differences between experimental and modelled values of the constant drying rate for each experiment were minimized by least squares method. Optimized values of b are also shown in Table 2.

Linear correlations ($R^2 > 0.99$) for b parameter with HPMC content for both thicknesses were found (Figure S1). Therefore, equations for the estimation of the constant drying rate depending on the air-drying temperature and HPMC content for each studied thickness, 0.50 and 0.25 cm, were obtained, Eqs. (6) and (7), respectively:

$$-\frac{dX}{dt} = 0.0002247\ \mathrm{T} - 0.0012\ \mathrm{C} - 0.0105 \tag{6}$$

$$-\frac{dX}{dt} = 0.0003350\ \mathrm{T} - 0.0019\ \mathrm{C} - 0.0123 \tag{7}$$

where T is the temperature (°C) and C is the HPMC content (% w/w).

Experiments showed that in the falling rate period, the drying rate decreased linearly from the critical point (X_c, k) to (0, 0), as previously was explained. That is, it started in the critical moisture of 0.38 kg water/kg d.s. Therefore, the obtained models for this period are those described in Eqs. (8) and (9) for 0.50 and 0.25 cm, respectively:

$$-\frac{dX}{dt} = \frac{(0.0002247\ T - 0.0012\ C - 0.0105)}{0.38}\ X = K\,X \tag{8}$$

$$-\frac{dX}{dt} = \frac{(0.0003350\ T - 0.0019\ C - 0.0123)}{0.38}\ X = K\,X \tag{9}$$

with X below X_c.

With the proposed models (involving only three parameters) it was

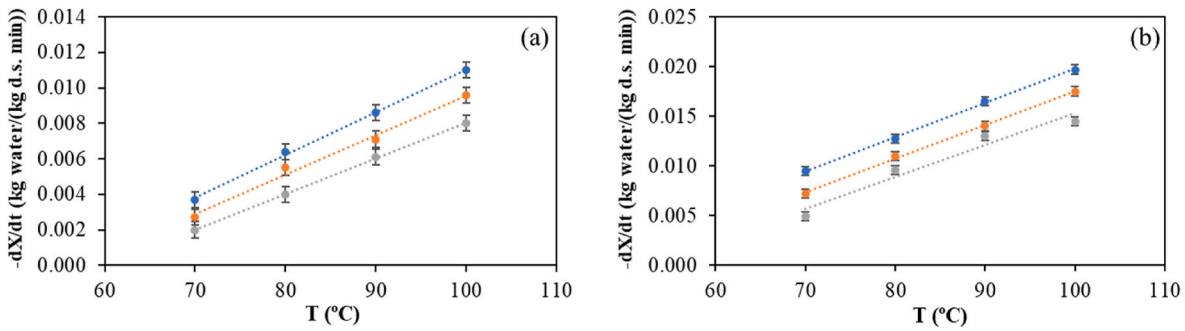

Fig. 3. Constant drying rate (k), Eq. (1), correlations with drying temperature at different HPMC content (% w/w, 1 ●, 2 ●, 3 ●) for different emulsion thickness (cm): (a) 0.50; (b) 0.25.

possible to obtain the drying rates (at fixed thickness) for any temperature and concentration of HPMC within the range of study, for both constant rate and falling rate periods. To validate the ability of these equations for predicting the drying kinetics, integration between conditions for both periods was performed, obtaining the expressions of Eq. (10) for the constant rate and Eq. (11) for the falling rate period:

$$X = X_0 - k\,t \tag{10}$$

$$X = X_c\, e^{-K\,(t_c - t)} \tag{11}$$

where X_0 (kg water/kg d.s) is the initial moisture content of emulsion, k (kg water/kg d.s min) is the drying rate value during the constant rate period given by Eqs. (6) and (7) at each tested thickness, t the drying time (min), shorter than the critical time t_c (time needed to reach the critical moisture X_c) in Eq. (10) and longer than t_c in Eq. (11), and K (1/min) is the constant for the falling rate period, estimated by Eqs. (8) and (9) for each tested thickness.

In Fig. 1, the experimental data of X *vs* t obtained from drying kinetics are represented together with modelled values from Eqs. (10) and (11). It can be observed that the proposed three-parameter model (besides X_c), which considers the simultaneous effect of air temperature and HPMC content of emulsion at fixed initial thickness, fitted the experimental data satisfactorily, with a maximum absolute error value of 3.4% and an average error lower than 1%. In general, the model predictions are slightly higher at the lowest tested temperature (70 °C). It is possible that water evaporation from the emulsion surface during the constant rate period at this temperature was slightly hindered by the lowest temperature of the air-emulsion interphase (corresponding to the wet bulb temperature of drying air), resulting in a lower heat driving force. In fact, this effect was much noticeable at 0.5 cm of thickness, where the specific surface is lower, and at 3% w/w of HPMC. It is necessary to consider that previous results found that gel temperature of HPMC (independently of the average molecular weight of HPMC depending only on its substitution degree) is around 61 °C (Montes et al., 2022). Consequently, the emulsions dried at 70 °C could have the formation of the layer delayed until this temperature was achieved in the surface and experimental data were slightly higher than modelled values in the falling rate period for these samples.

3.3. Effect of drying conditions and HPMC concentration on oleogel properties

Drying conditions conducted at 70 °C, regardless of HPMC concentration employed, did not lead to the formation of the oleogel due to the release of oil during the subsequent cutting and grinding phases. Therefore, it is necessary to operate at higher temperatures for using this biopolymer to obtain a stable oleogel. Moreover, oleogels containing 1% HPMC were not evaluated based on previous results. It has been demonstrated that HPMC concentrations exceeding 1% were necessary to yield stable oleogels with solid consistency (Espert et al., 2020).

3.3.1. Textural properties

Texture parameters of oleogels play a key role in their potential applications for the food industry, particularly regarding replacing and incorporating fats in final products. Specifically, oleogel hardness is of great importance since it directly impacts consumer acceptability and product shelf-life (Blake et al., 2018). Consequently, these results are the initial step towards validating these critical textural attributes.

In Fig. 4, oleogel hardness data is depicted, grouped by both emulsion thickness and HPMC concentration. After assessing hardness values across all batches, these values were within the range of 0.44–2.52 N. This hardness range partially agrees with those reported by Gómez-Estaca et al. (2019), who worked with mixtures of vegetable oils (olive and linseed) and fish oils gelled with ethyl-cellulose or beeswax, obtaining hardness in the interval 0.9–1.28 N. In other study, Espert et al. (2020), reported values of oleogel hardness of 1.71, 1.62 and 3.45 N for HPMC-sunflower oleogels, elaborated with 0.5%, 1% and 2% of oleogelator, respectively. The higher hardness reported by these authors for the oleogel prepared with 2% HPMC (3.45 N) compared to our highest value (1.23 N for 2% HPMC dried at 100 °C) may be attributed to differences in oleogelator viscosity (100 vs. 4000 cP).

After the GLM analysis, our findings showed that HPMC concentration ($F = 84.7$; $P < 0.001$) was the most important trait affecting oleogel maximum hardness, following by temperature ($F = 4.59$; $P = 0.018$) and emulsion thickness ($F = 1.44$; $P = 0.238$). No significant interactions were detected. The drying temperature had a lesser impact on oleogel hardness than HPMC concentration. As indicated before, tested temperatures exceeded the oleogelator gelling point, ensuring sufficient conditions for gelation.

Indeed, across all drying conditions (temperatures and thickness emulsion), an increase in HPMC concentration during oleogel formulation resulted in a significant ($P < 0.001$) rise in hardness (1.04 vs. 1.84 N for 2% and 3%, respectively). This finding agrees with previous studies indicating that higher oleogelator concentrations lead to increased oleogel hardness (Bascuas et al., 2020; Espert et al., 2020; Thakur et al., 2022). The higher concentration of biopolymer allows the formation of a more robust three-dimensional network, efficiently entrapping the oil. Conversely, lower concentrations of organogelator did not produce sufficient biopolymer interactions, resulting in an inadequate structure incapable of oil gelation.

The hardness of 2.52 N was achieved for oleogels formulated with 3% HPMC and dried at 90 °C with an emulsion thickness of 0.25 cm (Fig. 4a). Concerning drying temperature, oleogel hardness exhibited a significant increase ($P < 0.05$) as the temperature rose from 80 to 100 °C for both emulsion thickness assessed with 2% HPMC. However, this behaviour was not observed in the case of the HPMC concentration increased to 3%, particularly with an emulsion thickness of 0.5 cm,

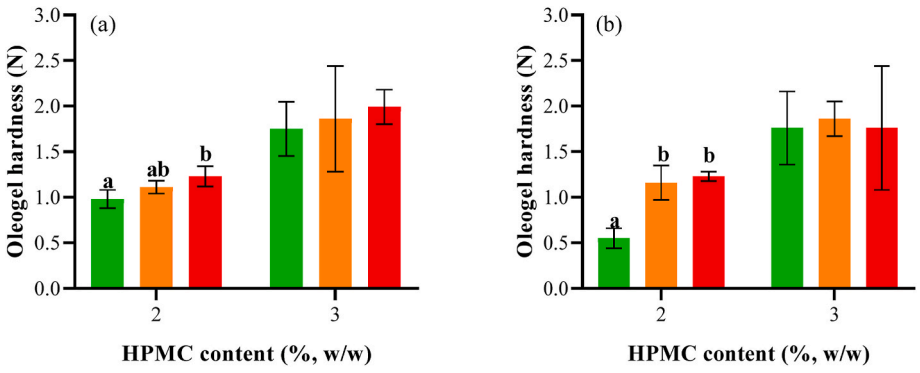

Fig. 4. Effect of drying temperature (°C, 80 ●,90 ▲,100 ■) on oleogel hardness for different HPMC content (% w/w) and emulsion thicknesses (cm): (a) 0.50 and (b) 0.25. The different letters in the error bars (a–c) indicate significant differences ($P < 0.05$) for a fixed HPMC concentration.

because of an increase in the population standard deviation. Hardness values were correlated with the total necessary work of compression and elasticity modulus. Therefore, these two textural traits exhibited a similar trend, and for the sake of brevity, detailed results for these parameters are not presented here.

3.3.2. Oil binding capacity

The OBC is a pivotal characteristic in determining the strength of an oleogel according to Doan et al. (2018). This parameter indicates the nature of the interaction between the oleogelator and the oil, particularly when the gel is subjected to mechanical stresses. Following a comprehensive GLM analysis, our findings have unveiled significant insights. The emulsion thickness ($F = 958.1$; $P < 0.001$) stood out as the primary factor influencing the OBC of the oleogel, followed by temperature ($F = 18.3$; $P < 0.001$) and HPMC concentration ($F = 1.3$; $P = 0.269$). The impact of emulsion thickness on OBC can be clearly observed in Fig. 5 (a and b). Oleogels dried under a thickness of 0.25 cm exhibited OBC values within the 79%–99% range. Conversely, an increase in emulsion thickness to 0.5 cm led to OBC values below 60%, regardless of temperature and HPMC concentration ($P > 0.05$).

Concerning batches drying at 0.25 cm emulsion thickness, drying temperature significantly affected the OBC for both 2% and 3% HPMC content ($P < 0.05$). As the temperature increased, the OBC decreased by 9.81 and 19.85% for 2% and 3% HPMC content, respectively. This phenomenon could be related to the shrinkage of colloidal materials as water is removed. As the migration of free water to the surface, soluble compounds accumulate on the dehydrated surface (Brennan & Grandison, 2012), producing the oleogel surface more impermeable to liquid flow and slowing down moisture removal. As the HPMC is partially water-soluble it is hypothesized that under higher drying temperatures, would cause its accumulation on the surface potentially explaining the reduced oil retention. This can also be related with the falling rate period of drying in which the formation and growth of this layer takes place. On one side, at higher temperature the layer is formed faster and on the other, as HPMC concentration increased, so did the capacity of the layer to impede water migration, hindering the stability of the oleogel obtained. It is worth noting that the literature suggests that oleogels with higher strength values should exhibit superior oil retention, thereby minimizing losses (Tanislav et al., 2022). However, this correlation was not observed in this study.

It is noteworthy that previous research has reported OBC values exceeding 97% using sunflower oil (Espert et al., 2020) soybean oil (Thakur et al., 2022), canola or linseed oil (Morales et al., 2023). In conclusion, oleogels for industrial applications need a high OBC as a critical parameter. Consequently, it can conclude that emulsion thicknesses greater than 0.25 cm during the drying process are not suitable for achieving oleogels with the target OBC.

3.3.3. Color features

Color plays a pivotal role in the sensory evaluation of novel products or ingredients as well as a key organoleptic factor for consumers. The L*, a* and b* values for each batch of oleogels are displayed in Figure S2. No significant differences were found between oleogels dried at different thicknesses. The lightness (L*) of the oleogel ranged from 25 to 35 at 2% and 3% of HPMC content. Temperature had a significant impact on L* ($P < 0.05$) of oleogels at 2% HPMC, increasing it from 27.6 to 34.4, for 80 and 100 °C, respectively. The a* values predominantly led towards negative values, ranging from −0.2 to −1.5 indicating a higher proportion of green hue. Overall, the importance of this trichromatic coordinate is lower for this type of oleogels. It should be noted that increasing drying temperature significantly ($P < 0.05$) reduced the b* value from 2.09 to 0.52. This decrease may be related to the potential impact of temperature on oxidation, although lipid oxidation assessments were not carried out to confirm this hypothesis. Conversely, it was observed that the increase in temperature did not significantly ($P > 0.05$) affect b* in oleogels of 3% HPMC.

3.4. Oleogel stability

To assess the stability of oleogels, the emulsion thickness was maintained at 0.25 cm during the drying process, based on the prior results (particularly, OBC results). Time and temperature conditions during oleogel storage were fixed for 20 days and room temperature (20 °C), respectively.

After the GLM analysis, our findings showed that storage time ($F = 26.9$; $P < 0.001$) was the most important trait affecting oleogel maximum hardness, following by HPMC content ($F = 8.2$; $P = 0.007$) and temperature ($F = 0.27$; $P = 0.759$). No significant interactions were detected among the three independent variables.

For all HPMC content and drying temperatures, storage time consistently increased oleogel hardness. Notably, the results for oleogels of 2% HPMC showed greater dispersion, which did not permit to reach statistical significance among oleogels by temperature effect in opposite to those elaborated with 3% HPMC (Fig. 6).

The GLM analysis for OBC highlighted that storage time ($F = 144.8$; $P < 0.001$) was the most important independent factor, followed by temperature ($F = 57.6$; $P < 0.001$) and HPMC content ($F = 13.31$; $P = 0.001$), as depicted in Fig. 7 (a and b). After 20 days of storage at room temperature (20 °C), mean OBC percentages of 99.76 ± 0.23 and 99.59 ± 0.45 were obtained for oleogels with 2% and 3% HPMC, respectively. This demonstrates a positive impact of storage time on oil retention, particularly in samples dried at 100 °C. These fresh samples (at day 0) exhibited significant ($P > 0.05$) lower oil retention due to an incompletely developed structure, needing additional time to enhance their OBC. On the contrary, it can be observed in Fig. 7, that those oleogels dried at a below temperature of 100 °C, provided an exceptional OBC from the outset, which remained consistent and did not diminish over

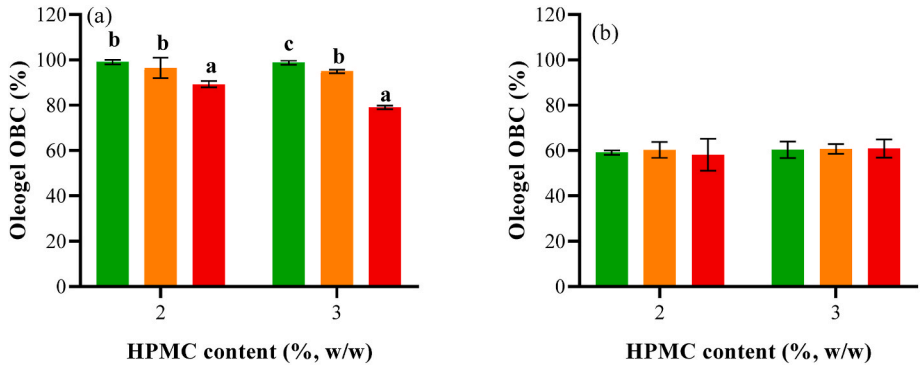

Fig. 5. Effect of drying temperature (°C, 80 ●,90 ▲,100 ■) on oleogel OBC for different HPMC content (% w/w) and emulsion thicknesses (cm): (a) 0.50 and (b) 0.25). The different letters in the error bars (a–c) indicate significant differences ($P < 0.05$) for a fixed HPMC concentration.

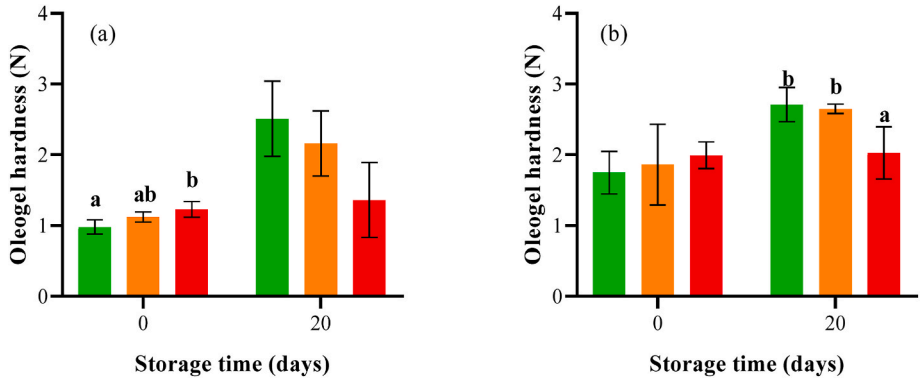

Fig. 6. Effect of drying temperature (°C, 80 ●,90 ▲,100 ■) on oleogel hardness for different HPMC content (%, w/w): (a) 2% and (b) 3%, on fresh and stored samples. The different letters in the error bars (a–c) indicate significant differences ($P < 0.05$) for a fixed HPMC concentration.

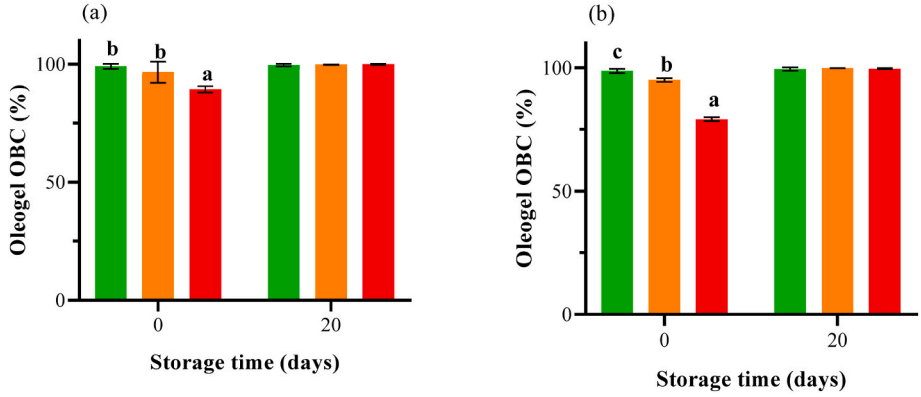

Fig. 7. Effect of drying temperature (°C, 80 ●,90 ▲,100 ■) on oleogel OBC for different HPMC content (%, w/w): (a) 2% and (b) 3%, on fresh and stored samples. The different letters in the error bars (a–c) indicate significant differences ($P < 0.05$) at fixed storage day.

the assessed storage time. Therefore, our findings suggest that stored oleogels at room temperature (20 °C) for at least 20 days could be seamlessly integrated into food formulations, without significant oil losses.

Concerning color parameters, storage time was the most critical factor, followed by HPMC content and drying temperature in agreement with previous results for oleogel hardness and OBC (Figure S2). To provide a more robust assessment of color changes, the absolute color difference (ΔE) (Mokrzycki & Tatol, 2011) during the storage period was evaluated (Fig. 8). In this study, ΔE values of 25.2 and 24.1 were obtained in oleogels of 2% HPMC dried at 90 and 100 °C, whereas slightly lower values of 17.8 and 18.1 were observed at the same temperatures and with 3% HPMC content. In contrast, at the lower temperature of 80 °C, ΔE did not exceed 2.0.

After the storage time, regardless of the temperature and HPMC content, the lightness of all oleogels decreased, indicating the development of a darker color associated to oxidative processes (although further tests are required to confirm this hypothesis. Thus, storage time could be considered relevant in the context of this color parameter, as higher L* values indicate a more luminous appearance in oleogel. In contrast, the redness (a*) and yellowness (b*) indices increased in all cases over time. Overall, b* has more importance in oils from oilseeds, although the refined oil used in our study did not exhibit a pronounced yellowness index ($b^* = 1.84 \pm 0.02$). Additionally, it was observed that drying temperature consistently had a significant effect ($P < 0.05$) on all trichromatic coordinates for each of the six batches analyzed, although the variations were minor (Figure S2).

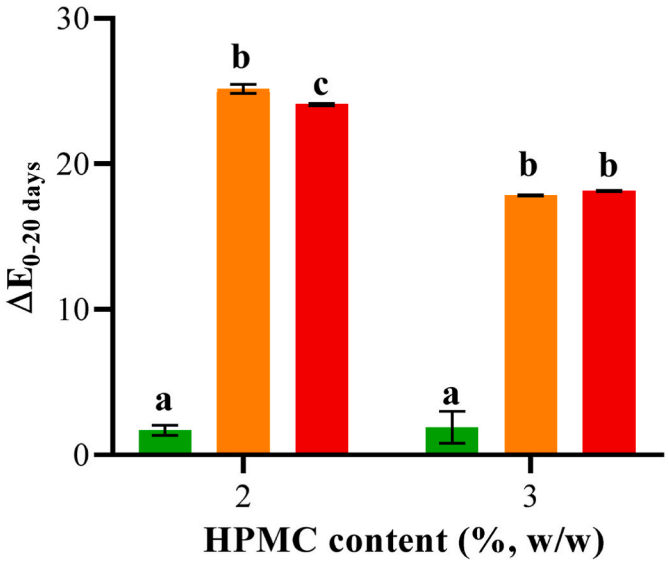

Fig. 8. Absolute color difference, ΔE, between fresh (0 days) and stored (20 days) oleogels produced at different drying temperature (°C, 80 ●,90 ▲,100 ■) and HPMC content. The different letters in the error bars (a–c) indicate significant differences ($P < 0.05$) at fixed storage day.

4. Conclusions

The water removal from emulsions showed an initial constant drying rate period meanwhile liquid water was present on the surface of the emulsion. Constant drying rate depended linearly on air temperature and HPMC content. At critical moisture content (0.38 kg water/kg dry solid) a gelled solid was formed at the surface constituting a barrier to moisture transport and its growth gave place the falling drying rate period. In this period, drying rate decreased linearly with moisture content. A 3-parameter model was successfully tested to simulate drying kinetics (including both drying periods) of emulsions as function of air temperature and HPMC content at a fixed thickness.

A threshold HPMC content of 2% w/w and temperatures above 80 °C were necessary to obtain stable and developed structured oils. Overall, oleogel hardness increased with increasing HPMC content and drying temperature (this latter with lesser impact). Initial thickness was critical in relation to oil binding capacity (OBC) and values smaller than 0.50 cm are recommendable to obtain satisfactory results. High drying temperatures decreased OBC values and HPMC content above 2% w/w did not improve this relevant parameter.

Oleogels hardness increased during storage (20 days) with the highest hardening in samples dried at the lowest temperature (80 °C) and low (2% w/w) HPMC content. On the other hand, OBC parameter was constant or increased after storage and color was practically invariant in samples dried at 80 °C, but dramatically increased when higher drying temperatures were employed independently of HPMC content.

Finally, it would be necessary to include studies in future works on the oxidation of the oil depending on the drying conditions employed and also, to perform structural studies to elucidate when interactions between the components are promoted in each drying stage.

CRediT authorship contribution statement

M.Y. Saavedra: Investigation, Formal analysis. **L. Montes:** Writing – review & editing, Formal analysis. **D. Franco:** Writing – review & editing, Writing – original draft, Methodology, Conceptualization. **A. Franco-Uría:** Writing – review & editing, Writing – original draft, Methodology, Conceptualization. **R. Moreira:** Writing – review & editing, Writing – original draft, Validation, Methodology, Conceptualization.

Declaration of competing interest

The authors declare that they have no known competing financial interests or personal relationships that could have appeared to influence the work reported in this paper.

Data availability

Data will be made available on request.

Acknowledgements

This work was funded by MCIN/AEI/10.13039/501100011033 and, as appropriate, by the "European Union NextGenerationEU/PRTR (grant CNS2022-135217).

Appendix A. Supplementary data

Supplementary data to this article can be found online at https://doi.org/10.1016/j.fbio.2024.103912.

References

Abdolmaleki, K., Alizadeh, L., Nayebzadeh, K., Hosseini, S. M., & Shahin, R. (2020). Oleogel production based on binary and ternary mixtures of sodium caseinate, xanthan gum, and guar gum: Optimization of hydrocolloids concentration and drying method. *Journal of Texture Studies, 51*, 290–299. https://doi.org/10.1111/jtxs.12469

Alizadeh, L., Abdolmaleki, K., Nayebzadeh, K., & Hosseini, S. M. (2020). Oleogel fabrication based on sodium caseinate, hydroxypropyl methylcellulose, and beeswax: Effect of concentration, oleogelation method, and their optimization. *Journal of the American Oil Chemists' Society, 97*, 485–496. https://doi.org/10.1002/aocs.12341

Álvarez, M. D., Cofrades, S., Espert, M., Salvador, A., & Sanz, T. (2021). Thermorheological characterization of healthier reduced-fat cocoa butter formulated by substitution with a hydroxypropyl methylcellulose (HPMC)-based oleogel. *Foods, 10*, 793. https://doi.org/10.3390/foods10040793

Bascuas, S., Hernando, I., Moraga, G., & Quiles, A. (2020). Structure and stability of edible oleogels prepared with different unsaturated oils and hydrocolloids. *International Journal of Food Science and Technology, 55*, 1458–1467. https://doi.org/10.1111/ijfs.14469

Bascuas, S., Morell, P., Hernando, I., & Quiles, A. (2021). Recent trends in oil structuring using hydrocolloids. *Food Hydrocolloids, 118*, Article 106612. https://doi.org/10.1016/j.foodhyd.2021.106612

Blake, A. I., Toro-Vazquez, J. F., & Hwang, H. (2018). Wax oleogels. In A. Marangoni, & N. Garti (Eds.), *Edible oleogels structure and health implications* (pp. 133–172). Cambridge, MA, USA.

Brennan, J. G., & Grandison, A. S. (2012). *Food processing handbook*. Weinheim, Germany: Wiley-VCH.

Chen, X. W., & Yang, X. Q. (2019). Characterization of orange oil powders and oleogels fabricated from emulsion templates stabilized solely by a natural triterpene saponin. *Journal of Agricultural and Food Chemistry, 67*, 2637–2646. https://doi.org/10.1021/acs.jafc.8b04588

Doan, C. D., Tavernier, I., Okuro, P. K., & Dewettinck, K. (2018). Internal and external factors affecting the crystallization, gelation and applicability of wax-based oleogels in food industry. *Innovative Food Science and Emerging Technologies, 45*, 42–52. https://doi.org/10.1016/j.ifset.2017.09.023

Espert, M., Hernández, M. J., Sanz, T., & Salvador, A. (2021). Reduction of saturated fat in chocolate by using sunflower oil-hydroxypropyl methylcellulose based oleogels. *Food Hydrocolloids, 120*, Article 106917. https://doi.org/10.1016/j.foodhyd.2021.106917

Espert, M., Salvador, A., & Sanz, T. (2020). Cellulose ether oleogels obtained by emulsion-templated approach without additional thickeners. *Food Hydrocolloids, 109*, Article 106085. https://doi.org/10.1016/j.foodhyd.2020.106085

Gatti, R. C., Liang, J., Velichevskaya, A., & Zhou, M. (2019). Sustainable palm oil may not be so sustainable. *Science of the Total Environment, 652*, 48–51. https://doi.org/10.1016/j.scitotenv.2018.10.222

Goavec, M., Rodts, S., Gaudefroy, V., Coquil, M., Keita, E., Goyon, J., Chateau, X., & Coussot, P. (2018). Strengthening and drying rate of a drying emulsion layer. *Soft Matter, 14*, 8612–8626. https://doi.org/10.1039/C8SM01490F

Gómez-Estaca, J., Herrero, A., Herranz, B., Álvarez, M., Jiménez-Colmenero, F., & Cofrades, S. (2019). Characterization of ethyl cellulose and beeswax oleogels and their suitability as fat replacers in healthier lipid pâtés development. *Food Hydrocolloids, 87*, 960–969. https://doi.org/10.1016/j.foodhyd.2018.09.029

Huang, L., Cai, Y., Fang, D., Su, J., Zhao, M., Zhao, Q., & Van der Meeren, P. (2023). Formation and characterization of oleogels derived from emulsions: Evaluation of polysaccharide ratio and emulsification method. *Food Hydrocolloids, 142*, Article 108844. https://doi.org/10.1016/j.foodhyd.2023.108844

Jiang, Y., Liu, L., Wang, B., Sui, X., Zhong, Y., Zhang, L., Mao, Z., & Xu, H. (2018). Cellulose-rich oleogels prepared with an emulsion-templated approach. *Food Hydrocolloids, 77*, 460–464. https://doi.org/10.1016/j.foodhyd.2017.10.023

Jung, I., Schroeter, B., Plazzotta, S., De Berardinis, L., Smirnova, I., Gurikov, P., & Manzocco, L. (2023). Oleogels from mesoporous whey and potato protein based aerogel microparticles: Influence of microstructural properties on oleogelation ability. *Food Hydrocolloids, 142*, Article 108758. https://doi.org/10.1016/j.foodhyd.2023.108758

Korese, J. K., Achaglinkame, M. A., & Chikpah, S. K. (2021). Effect of hot air temperature on drying kinetics of palmyra (*Borassus aethiopum* Mart.) seed-sprout fleshy scale slices and quality attributes of its flour. *Journal of Agriculture and Food Research, 6*, Article 100249. https://doi.org/10.1016/j.jafr.2021.100249

Kowalski, S. J., Mierzwa, D., & Stasiak, M. (2017). Ultrasound-assisted convective drying of apples at different process conditions. *Drying Technology, 35*, 939–947. https://doi.org/10.1080/07373937.2016.1239631

Li, X., Guo, G., Zou, Y., Luo, J., Sheng, J., Tian, Y., & Li, J. (2023). Development and characterization of walnut oleogels structured by cellulose nanofiber. *Food Hydrocolloids, 142*, Article 108849. https://doi.org/10.1016/j.foodhyd.2023.108849

Manzoor, S., Masoodi, F. A., Naquash, F., & Rashid, R. (2022). Oleogels: Promising alternatives to solid fats for food applications. *Food Hydrocolloids for Health, 2*, Article 100058. https://doi.org/10.1016/j.fhfh.2022.100058

Mokrzycki, W., & Tatol, M. (2011). Color difference Delta E - a survey. *Machine Graphics and Vision, 20*, 383–411.

Montes, L., Rosell, C. M., & Moreira, R. (2022). Rheological properties of corn starch gels with the addition of hydroxypropyl methylcellulose of different viscosities. *Frontiers in Nutrition, 9*, Article 866789. https://doi.org/10.3389/fnut.2022.866789

Moradabbasi, M., Goli, S. A. H., & Fayaz, G. (2022). Effect of biopolymers concentration and drying methods on physicochemical properties of emulsion-templated oleogel.

Journal of Food Science and Technology, 59, 1994–2003. https://doi.org/10.1007/s13197-021-05214-1

Morales, E., Iturra, N., Contardo, I., Quilaqueo, M., Franco, D., & Rubilar, M. (2023). Fat replacers based on oleogelation of beeswax/shellac wax and healthy vegetable oils. LWT-. *Food Science and Technology, 185*, Article 115144. https://doi.org/10.1016/j.lwt.2023.115144

Oh, I. K., & Lee, S. (2018). Utilization of foam structured hydroxypropyl methylcellulose for oleogels and their application as a solid fat replacer in muffins. *Food Hydrocolloids, 77*, 796–802. https://doi.org/10.1016/j.foodhyd.2017.11.022

Okuro, P. K., Tavernier, I., Bin Sintang, M. D., Skirtach, A. G., Vicente, A. A., Dewettinck, K., & Cunha, R. L. (2018). Synergistic interactions between lecithin and fruit wax in oleogel formation. *Food & Function, 9*, 1755–1767. https://doi.org/10.1039/c7fo01775h

Pan, H., Xu, X., Qian, Z., Cheng, H., Shen, X., Chen, S., & Ye, X. (2021). Xanthan gum-assisted fabrication of stable emulsion-based oleogel structured with gelatin and proanthocyanidins. *Food Hydrocolloids, 115*, Article 106596. https://doi.org/10.1016/j.foodhyd.2021.106596

Patel, A. R. (2015). *Alternative Routes to oil structuring*. Springer. https://doi.org/10.1007/978-3-319-19138-6

Patel, A. R., Cludts, N., Sintang, M. D. B., Lesafferb, A., & Dewettinck, K. (2014). Edible oleogels based on water soluble food polymers: Preparation, characterization and potential application. *Food & Function, 5*, 2673–3028. https://doi.org/10.1039/c4fo00624k

Perfetti, G., Alphazan, T., Wildeboer, W. J., & Meesters, G. M. H. (2012). Thermo-physical characterization of Pharmacoat® 603, Pharmacoat® 615 and Mowiol® 4-98. *Journal of Thermal Analysis and Calorimetry, 109*, 203–215. https://doi.org/10.1007/s10973-011-1664-9

Puscas, A., Muresan, V., Socaciu, C., & Muste, S. (2020). Oleogels in food: A review of current and potential applications. *Foods, 9*, 70. https://doi.org/10.3390/foods9010070

Qiu, C., Huang, Y., Li, A., Ma, D., & Wang, Y. (2018). Fabrication and characterization of oleogel stabilized by gelatin-polyphenol-polysaccharides nanocomplexes. *Journal of Agricultural and Food Chemistry, 66*, 13243–13252. https://doi.org/10.1021/acs.jafc.8b02039

Singh, N. J., & Pandey, R. K. (2012). Convective air drying characteristics of sweet potato cube (*Ipomoea batatas L.*). *Food and Bioproducts Processing, 90*, 317–322. https://doi.org/10.1016/j.fbp.2011.06.006

Tanislav, A., Puscas, A., Paucean, A., Muresan, A., Semeniuc, C., Muresan, V., & Mudura, E. (2022). Evaluation of structural behavior in the process dynamics of oleogel-based tender dough products. *Gels, 8*, 317. https://doi.org/10.3390/gels8050317

Thakur, D., Singh, A., Prabhakar, P. K., Meghwal, M., & Upadhyay, A. (2022). Optimization and characterization of soybean oil-carnauba wax oleogel. *LWT–Food Science and Technology, 157*, Article 113108. https://doi.org/10.1016/j.lwt.2022.113108

Wang, Q., Espert, M., Larrea, V., Quiles, A., Salvador, A., & Sanz, T. (2023). Comparison of different indirect approaches to design edible oleogels based on cellulose ethers. *Food Hydrocolloids, 134*, Article 108007. https://doi.org/10.1016/j.foodhyd.2022.108007

Xiao, H. W., Bai, J. W., Xie, L., Sun, D. W., & Gao, Z. J. (2015). Thin-layer air impingement drying enhances drying rate of American ginseng (*Panax quinquefolium L.*) slices with quality attributes considered. *Food and Bioproducts Processing, 94*, 581–591. https://doi.org/10.1016/j.fbp.2014.08.008

Xu, Y., Sun, H., Lv, J., Wang, Y., Zhang, Y., & Wang, F. (2023). Effects of polysaccharide thickening agent on the preparation of walnut oil oleogels based on methylcellulose: Characterization and delivery of curcumin. *International Journal of Biological Macromolecules, 232*, Article 123291. https://doi.org/10.1016/j.ijbiomac.2023.123291

Zheng, S., Lu, M., Xiao, J., Zhang, X., Li, J., Zhang, H., Zhang, C., Cao, Y., & Lan, Y. (2023). A novel strategy for preparation of rice bran protein oleogels based on high internal phase emulsion template. *Journal of the Science of Food and Agriculture, 103*, 5717–5726. https://doi.org/10.1002/jsfa.12672